

Article

Microstructures and Tensile Properties of Al–Cu Matrix Composites Reinforced with Nano-Sized SiC_p Fabricated by Semisolid Stirring Process

Feng Qiu ^{1,3}, Xiang Gao ¹, Jian Tang ¹, Yu-Yang Gao ¹, Shi-Li Shu ², Xue Han ³, Qiang Li ¹ and Qi-Chuan Jiang ^{1,*}

¹ Key Laboratory of Automobile Materials, Ministry of Education and Department of Materials Science and Engineering, Jilin University, Renmin Street NO. 5988, Changchun 130025, China; qiufeng@jlu.edu.cn (F.Q.); xianggao15@mails.jlu.edu.cn (X.G.); xxe8198458@163.com (J.T.); gaoyy14@mails.jlu.edu.cn (Y.-Y.G.); liqiang15@mails.jlu.edu.cn (Q.L.)

² State Key Laboratory of Luminescence and Applications, Changchun Institute of Optics, Fine Mechanics and Physics, Chinese Academy of Sciences, Changchun 130012, China; shushili@ciomp.ac.cn

³ Department of Mechanical Engineering, Oakland University, Rochester, MI 48309, USA; xhan@oakland.edu

* Correspondence: jiangqc@jlu.edu.cn; Tel./Fax: +86-431-85094699

Academic Editor: Manoj Gupta

Received: 29 December 2016; Accepted: 3 February 2017; Published: 8 February 2017

Abstract: The nano-sized SiC_p/Al–Cu composites were successfully fabricated by combining semisolid stirring with ball milling technology. Microstructures were examined by an olympus optical microscope (OM), field emission scanning electron microscope (FESEM) and transmission electron microscope (TEM). Tensile properties were studied at room temperature. The results show that the α-Al dendrites of the composites were strongly refined, especially in the composite with 3 wt. % nano-sized SiC_p, of which the morphology of the α-Al changes from 200 μm dendritic crystal to 90 μm much finer equiaxial grain. The strength and ductility of the composites are improved synchronously with the addition of nano-sized SiC_p particles. The as-cast 3 wt. % nano-sized SiC_p/Al–Cu composite displays the best tensile properties, i.e., the yield strength, ultimate tensile strength (UTS) and fracture strain increase from 175 MPa, 310 MPa and 4.1% of the as-cast Al–Cu alloy to 220 MPa, 410 MPa and 6.3%, respectively. The significant improvement in the tensile properties of the composites is mainly due to the refinement of the α-Al dendrites, nano-sized SiC_p strengthening, and good interface combination between the SiC_p and Al–Cu alloys.

Keywords: nano-sized SiC_p; aluminum matrix composites; mechanical properties; microstructures

1. Introduction

In the past decades, particulate reinforced aluminum matrix composites (AMCs) have attracted much attention in the field of structural and functional materials [1–4]. SiC_p reinforced AMCs have been a hot research issue in recent years because of their excellent properties such as low density, high tensile strength, high elastic modulus and wear resistance, etc. [5–7]. For example, SiC_p reinforced AMCs are used for engine piston, and heat sink [8,9]. Compared with traditional micron-sized SiC_p/Al composites, the higher tensile strength and good ductility of the nano-sized SiC_p/Al composites entitle them to have more competitive ability for advanced structural applications such as in automotive and aerospace industries and the military [10]. In the past decades, several processing techniques have been developed for fabricating Al matrix composites reinforced with nano-sized particles such as high-energy milling, powder metallurgy, and nano-sintering, and liquid-state solidification processing (e.g., stir casting) [11–19]. In these techniques, the semisolid stirring process has some important

advantages such as low cost, capability of producing products with complex shapes, and processing simplicity [14].

Al–Si and Al–Mg alloys are the usually used matrix phase in nano-sized SiC_p /Al composites [10,16,20,21]. Xiong et al. [10] fabricated 14 vol. % nano-sized SiC_p /Al–Mg composites. They reported that the ultimate tensile strength increased from 223 MPa to 286 MPa, while the ductility decreased from 4.8% to 3.9%. Hamedan et al. [16] produced 1.0 wt. % nano-sized SiC_p /Al356 composite and reported that the ultimate tensile strength of the composite increased from 140 MPa to 173 MPa, while the ductility decreased slightly from 6.1% to 5.38%. Compared to the Al–Si and Al–Mg alloys, the Al–Cu alloys can offer some good mechanical properties. For instance, a previous study by us has shown that the tensile strength and elongation increased by 26% and 50% respectively, for the modified Al–Cu alloys compared with unmodified alloy [22]. Moreover, we also found that the corrosion resistance of modified Al–Cu alloy had an improvement compared with the unmodified one [23]. However, to the best of our knowledge, so far, because there is no chemical affinity between the Cu element and SiC_p , and the Cu element can also not improve the wettability between the aluminum matrix and SiC_p [24], the Al–Cu alloys were rarely used as a matrix in the nano-sized SiC_p /Al composites in stir casting. It is believed that if the nano-sized SiC_p /Al–Cu composites with uniform distribution SiC_p and clean interface between the SiC_p and Al–Cu alloys could be successfully fabricated, the composites will exhibit excellent mechanical properties, which are very important for application in the automotive and aircraft industries.

In this paper, the nano-sized SiC_p /Al–Cu composites were fabricated by combining semisolid stirring with ball milling technology. Semisolid stirring can suppress the interfacial reaction due to the low stirring temperature [19]. The usage of precursor powders fabricated by the mix of the nano-sized SiC_p and alloy powders using mechanical ball milling is of benefit to the dispersion of the nano-sized SiC_p in the matrix due to the disruption of the agglomerate nano-sized SiC_p clusters in advance. The microstructures and tensile properties of the synthesized composites were investigated, and the strengthening mechanism was discussed. We expect that such knowledge would provide guidance for the fabrication and application of the nano-sized SiC_p /Al–Cu composites.

2. Experimental Procedure

The Al–Cu alloy with a composition of (wt. %): 5.0 Cu, 0.8 Mn, 0.7 Fe, 0.5 Mg, 0.5 Si, 0.25 Zn, 0.15 Ti, 0.1 Cr and Al (balance) was used as the matrix. The nano-sized SiC_p , with a purity of 99.9 wt. % and ~60 nm in diameter, were used as the reinforced particles. The morphology of the raw nano-sized SiC_p particles is shown in Figure 1a. If the agglomerate nano-sized SiC_p clusters are added into the melt directly, it is difficult for semisolid stirring to break the clustering and disperse the nano-sized particles uniformly. Figure 1b shows the Al–Cu alloy powders (99% pure) with average sizes of about 10 μm , their composition is the same as the Al–Cu alloy matrix. Figure 1c,d shows the precursor powders which are fabricated by the mix of the calculated nano-sized SiC_p and Al–Cu alloy powders using mechanical ball milling with ZrO_2 balls at the speed of 150 r/min for 50 h. Figure 1d is the a high magnification of the rectangular area in Figure 1c. It could be found that most of the nano-sized SiC_p display a relatively uniform distribution in each individual composite particle surface. The ball to powder weight ratio was 8:1. During melting, Al–Cu alloy was melted at 933 K in air using an electricity resistant furnace and then cooled to 873 K at which point the matrix alloy was in semi-solid condition. The temperature range for the Al–Cu alloy used in this study to be in the semi-solid condition is 813 K–903 K. Then, the precursor powder was added into the molten metal after stirring the molten metal with a graphite stirrer at the speed of 500 r/min. After that, the melt was poured into a preheated steel die. After the casting process, the Al–Cu alloy and the composites were homogenised for 10 h at 758 K in order to avoid segregation. The materials were extruded to the batten shaped samples with the help of a 200-ton hydraulic press at 773 K with the extrusion ratio of 16. Before the tensile test, all the extruded samples underwent the T6 heat treatment (solutionized at 773 K for 2 h and aged at 433 K for 18 h).

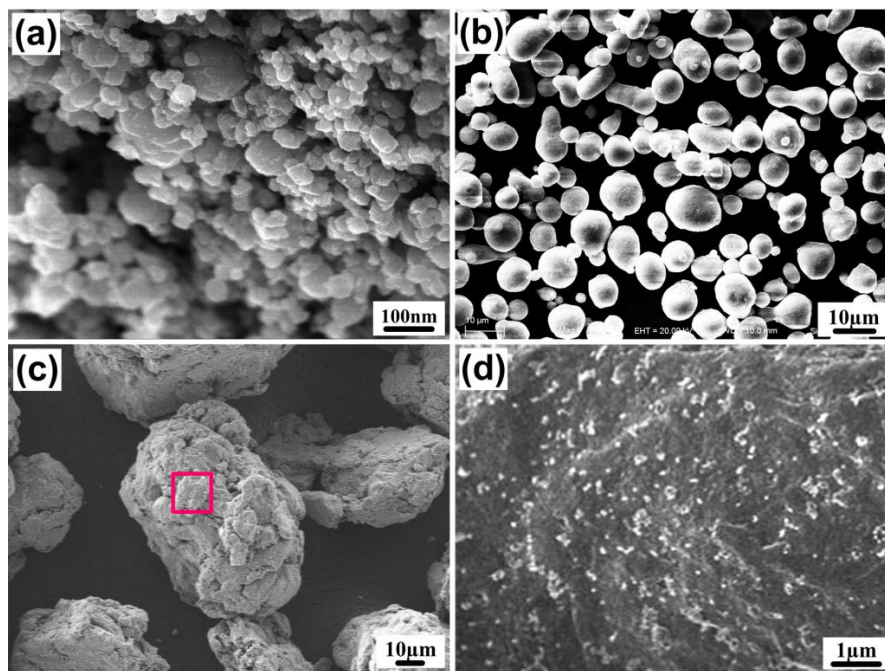


Figure 1. SEM images of morphologies of the raw (a) nano-sized SiC particles and (b) Al–Cu alloy powders; FESEM (field emission SEM) images of (c) nano-sized SiC_p/Al–Cu composite powders after ball milling; (d) high magnification of the area marked in (c).

Microstructures of the composites were examined by an Optical Microscope (Axio Imager A2m, Zeiss, Oberkochen, Germany) equipped with image analysis software and a camera; a computer was used for the OM observation and the quantitative measurements of microstructural features. The size of Al dendrites in every composite was measured from forty images taken at two magnifications, such as 50 \times , and 100 \times . Five samples of every composite were used to obtain the standard deviations (the error bars) plotted in Figure 2. Microstructures of the composites and morphologies of the raw nano-sized SiC particles and Al–Cu alloy powders were observed by field emission SEM (FESEM, JSM6700F, Tokyo, Japan) and SEM (Evo18, Carl Zeiss, Oberkochen, Germany).

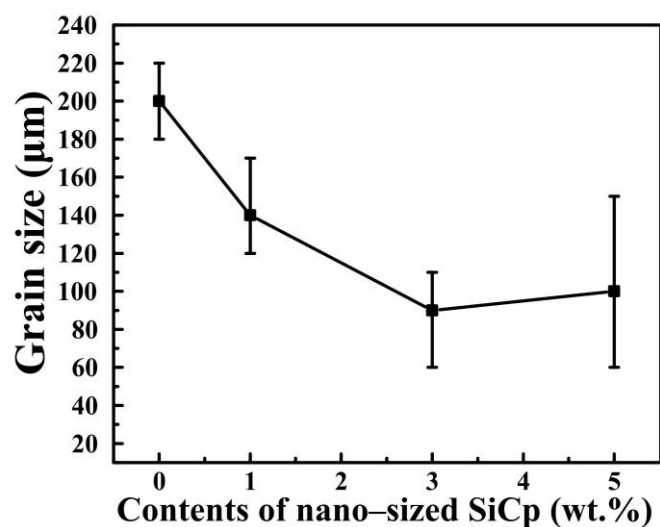


Figure 2. Grain sizes of α -Al in the cast Al–Cu alloy and nano-sized SiC_p/Al–Cu composites with different SiC_p contents.

The extruded samples were machined into dog-bone shaped tensile samples with a gauge cross section of 5.0 mm \times 2.5 mm and a gauge length of 30.0 mm. Tensile tests were conducted at room temperature by using a servo-hydraulic materials testing system (MTS, MTS 810, Minneapolis, MN, USA) at a constant strain rate of $3 \times 10^{-4} \text{ s}^{-1}$.

3. Results and Discussion

Figure 3 shows the as-cast microstructures of the Al–Cu alloy and nano-sized SiC_p /Al–Cu composites with the nominal content of 1 wt. %, 3 wt. %, 5 wt. % SiC_p . As shown in Figure 3a, the α -Al dendrites of the Al–Cu matrix alloy are coarse and their average size is about 200 μm . However, in the nano-sized SiC_p /Al–Cu composites, the α -Al dendrites are significantly refined by the addition of nano-sized SiC_p , as shown in Figure 3b–d. The refinement of the dendrite size is mainly due to some heterogeneous nucleation sites of the α -Al crystal provided by nano-sized particles during solidification, and the hindrance of the other added nano-sized SiC_p to the growth of α -Al dendrites during the solidification process. Figure 2 shows the size of dendrite in the nano-sized SiC_p /Al–Cu composites with different particle contents. In the 3 wt. % nano-sized SiC_p /Al–Cu composite, the morphology of α -Al changes from coarse dendritic grain to equiaxed grain with finer sizes of about 90 μm , which increases the boundary concentration in the Al matrix. The increase in the boundary concentration could be helpful to improve the tensile strength of metals or alloys due to the grain boundary playing a role as a barrier to the transmission of the dislocations. The as-cast microstructure of the composite with 5 wt. % SiC_p is similar to that with 3 wt. % SiC_p , although the sizes of the α -Al dendrites were uneven sizes of 60–150 μm (Figure 3d). In the composite with 5 wt. % SiC_p , the shape of Al dendrites became very non-uniform due to the agglomeration of nano-sized SiC_p particles. The hindrance effect of the nano-sized SiC_p on the α -Al dendrite growth is strong in the area of agglomeration of ceramic particles. On the contrary, the hindrance effect of the nano-sized SiC_p on the α -Al dendrite growth is weakened in the area of less ceramic particles. Thus, the difference in the size of the α -Al dendrites was probably due to the nonuniform dispersion of SiC_p when their contents reached 5 wt. %.

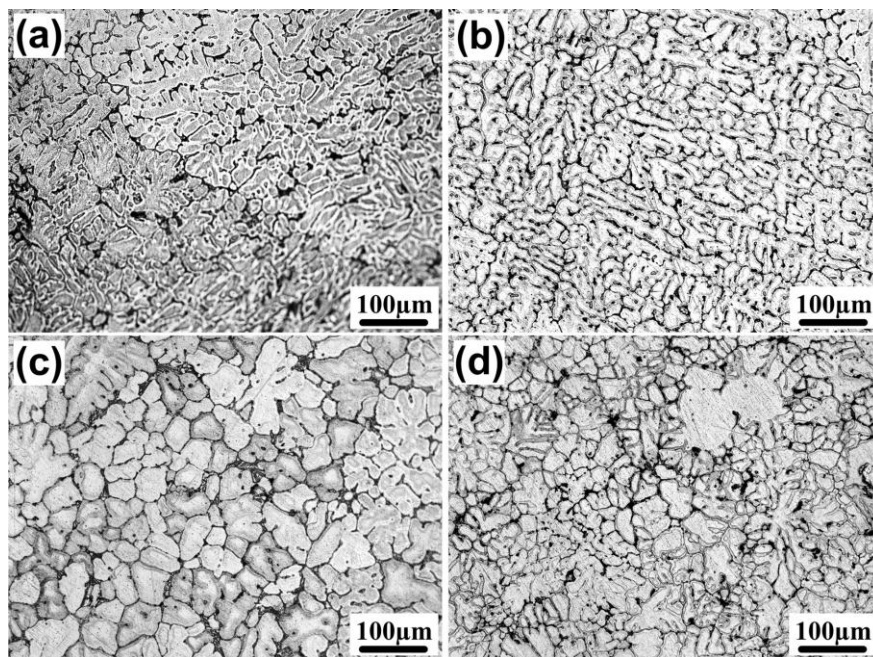


Figure 3. Cast microstructures of the nano-sized Al–Cu alloy and SiC_p /Al–Cu composites with different SiC_p contents; (a) Al–Cu alloy; (b) 1 wt. % SiC_p ; (c) 3 wt. % SiC_p ; (d) 5 wt. % SiC_p .

Figure 4 shows the engineering stress–strain curves of the cast Al–Cu alloy and nano-sized $\text{SiC}_p/\text{Al–Cu}$ composites, and Table 1 lists the detailed data of the tensile properties. As indicated, the strength and ductility of the composites (1 wt. % and 3 wt. %) are improved synchronously which is quite rare for the composites reinforced with ceramic particles, because in most reported works [11,14,20,21], the composites had a higher strength and lower ductility than the matrix alloy. The yield strength ($\sigma_{0.2}$), ultimate tensile strength (UTS) and fracture strain (ϵ) of the nano-sized $\text{SiC}_p/\text{Al–Cu}$ composites firstly increase and then decrease with the increase in the content of SiC_p . The 3 wt. % nano-sized $\text{SiC}_p/\text{Al–Cu}$ composite possesses the best tensile properties. The yield strength, UTS and fracture strain of the 3 wt. % $\text{SiC}_p/\text{Al–Cu}$ composite are 220 MPa, 410 MPa and 6.3%, which increase by 45 MPa (25.7%), 100 MPa (32.2%) and 2.2% (53.6%), respectively, compared to those of the as-cast Al–Cu alloy (175 MPa, 310 MPa and 4.1%).

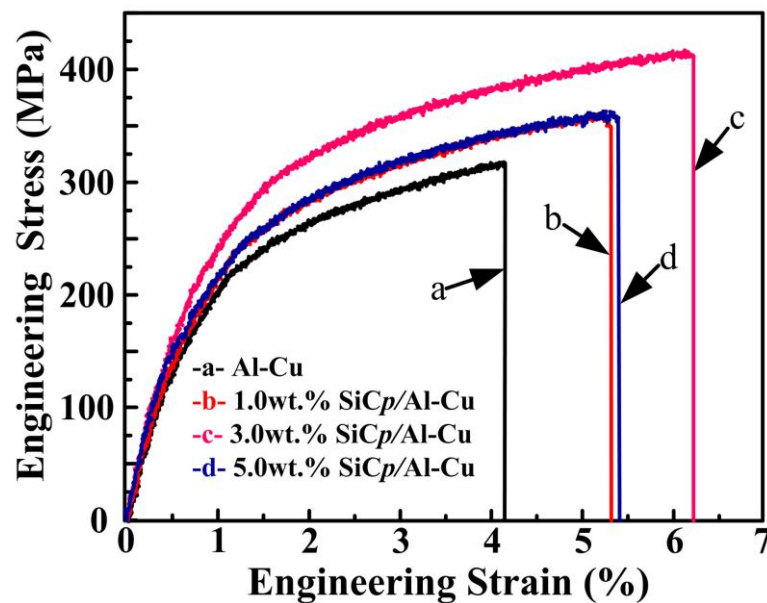


Figure 4. Tensile stress–strain curves of the cast Al–Cu alloy and nano-sized $\text{SiC}_p/\text{Al–Cu}$ composites with different SiC_p contents.

Table 1. Tensile properties of the as-cast Al–Cu alloy and nano-sized $\text{SiC}_p/\text{Al–Cu}$ composites with different SiC_p contents.

SiC_p (wt. %)	$\sigma_{0.2}$ (MPa)	σ_b (MPa)	ϵ (%)
0	175^{+8}_{-6}	310^{+11}_{-10}	$4.1^{+1.2}_{-0.5}$
1	185^{+7}_{-8}	358^{+12}_{-11}	$5.3^{+0.8}_{-0.7}$
3	220^{+10}_{-6}	410^{+14}_{-8}	$6.3^{+0.7}_{-0.5}$
5	190^{+5}_{-8}	362^{+5}_{-13}	$5.4^{+1.3}_{-1.6}$

Figure 5a–d shows the FESEM images of the 3 wt. % and 5 wt. % nano-sized $\text{SiC}_p/\text{Al–Cu}$ composite, and TEM micrographs of the 3 wt. % $\text{SiC}_p/\text{Al–Cu}$ composite. As indicated in Figure 5a,b, more evenly distributed nano-sized SiC_p particles in the 3 wt. % $\text{SiC}_p/\text{Al–Cu}$ composite are observed compared with the 5 wt. % $\text{SiC}_p/\text{Al–Cu}$ composite. However, in the 5 wt. % $\text{SiC}_p/\text{Al–Cu}$ composite as shown in Figure 5b, although there are some uniform distribution zones of nano-sized SiC_p , the agglomeration of particles can still be easily found, as shown in Figure 5d. In other words, more and more particles aggregate to form the clusters with the increase in the content of SiC_p , resulting in the quite uneven α -Al dendrites sizes and higher concentration of defects. As shown in Figure 5c, it is clearly seen that the nano-sized SiC particles dispersed inside the α -Al dendrite and the interface

between the SiC particles and matrix are good and clean without any contaminations, indicating the superiority of this fabrication technology.

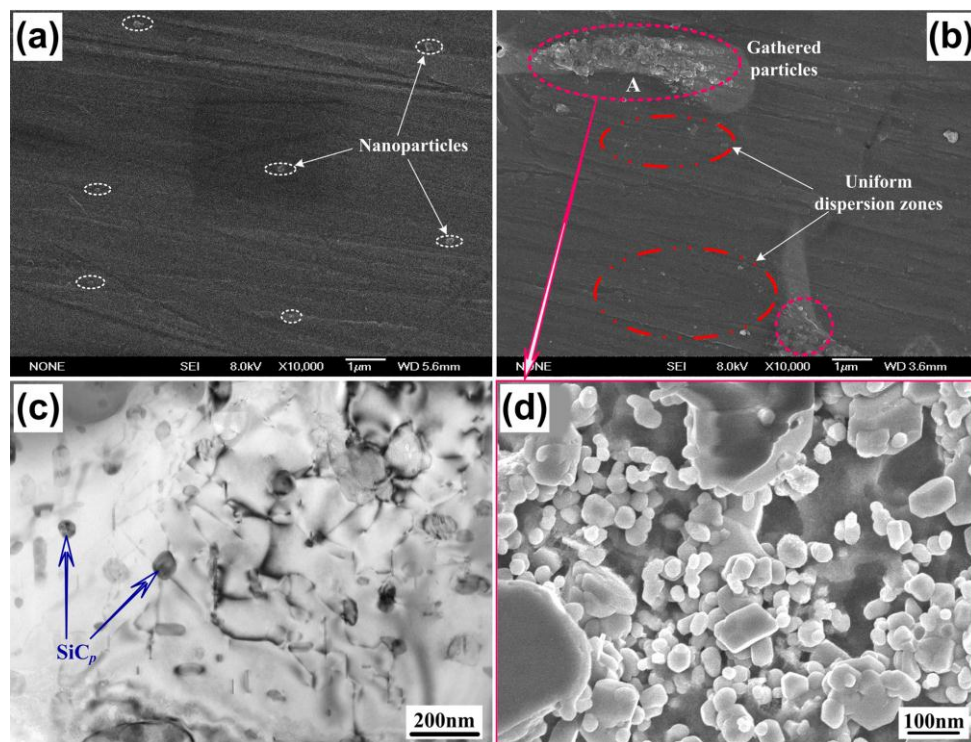


Figure 5. FESEM images of the (a) 3 wt. % and (b) 5 wt. % nano-sized SiC_p/Al-Cu composite; (c) TEM micrographs of the 3 wt. % SiC_p/Al-Cu composite; (d) the high magnification of area A in (b).

The significant improvement of the strength of the SiC_p/Al-Cu composites is mainly due to the refinement of the α -Al dendrites and the hindrance of the nano-sized SiC_p to the start and motion of dislocations in the matrix. Moreover, the significantly improved ductility of the nano-sized SiC_p/Al-Cu composites with a simultaneously increased tensile strength is derived from three factors:

- (i) Nano-sized reinforcement. Compared with micron-sized ceramic particles, the nano-sized ceramic particles used as reinforcement can not only possess higher tensile strength but also maintain good ductility, especially in the low contents [21]. Large reinforcement particles could give rise to cleavage in the particle due to the fact that they are acting as concentrators of stress, and lead to the formation of pits or cavities due to the loss of interphase cohesion. However, the smallest reinforcement particles usually do not initiate pits or cavities at the particle and bond well to the metal matrix [11].
- (ii) Dendrite refinement. The refinement of the α -Al dendrites will result in the increase in matrix dendrite boundaries. The finer the dendrite is, the more tortuous the grain boundaries are. Therefore, the crack propagation becomes more and more difficult and thus the composites can endure the larger plastic deformation before fracture.
- (iii) Suppression of interfacial reaction. It is known that the reaction between molten Al and SiC_p takes place easily in the temperature range from 675 °C to 900 °C, producing Al₄C₃ which is a brittle and unstable phase [12]. The presence of Al₄C₃ degrades the mechanical properties through crack propagation. In the present work, low stirring temperature (600 °C) during the semisolid stirring process can suppress the interfacial reaction effectively, which will be helpful to restrict the formation of the Al₄C₃ phase. The improved strength and cracking resistance of the interface bonding make the occurrence of the crack source cracking become more difficult.

Nano-sized particle strengthening, microstructure refinement, and good interface between reinforcement and matrix with no brittle intermetallics can be responsible for the significant improvement in the mechanical properties of the nano-sized SiC_p/Al–Cu composites. Hence, the nano-sized SiC_p/Al–Cu composites showed high plasticity and strength. However, the properties of the composite with high content nano-sized SiC_p particles could be weakened because this composite resulted in more agglomeration of the SiC_p and higher concentration of defects. More severe agglomeration of SiC_p could not lead to the matrix being completely wrapped up by the particles and thus result in the debonding of the interface. Moreover, micro-porosity and other defects around the SiC_p clusters presented in the composites become the cracking source during the plastic deformation. The above analyses imply that the embrittlement of the composites resulting from micro-porosity and defects results in the decrease in strength and ductility of the 5 wt. % SiC_p/Al–Cu.

4. Conclusions

The nano-sized SiC_p/Al–Cu composites with contents of 1 wt. %, 3 wt. %, 5 wt. % SiC_p were successfully fabricated by combining semisolid stirring with ball milling technology. The α -Al dendrites are significantly refined due to the addition of nano-sized SiC_p. The refinement of the dendrite size is mainly attributed to some nano-sized particles providing some heterogeneous nucleation sites of the α -Al crystal, and the hindrance of the other added nano-sized SiC_p to the growth of α -Al dendrites during the solidification process. The strength and ductility of the composites are improved synchronously with the addition of nano-sized SiC_p particles. The 3 wt. % nano-sized SiC_p/Al–Cu composite displays the best comprehensive tensile properties, i.e., the yield strength, UTS and fracture strain increase from 175 MPa, 310 MPa and 4.1% of the as-cast Al–Cu alloy to 220 MPa, 410 MPa and 6.3%, respectively. Nano-sized particle strengthening, microstructure refinement, and a good interface between reinforcement and the matrix with no brittle intermetallics can be responsible for the significant improvement in the mechanical properties of the nano-sized SiC_p/Al–Cu composites.

Acknowledgments: The National Natural Science Foundation of China (NNSFC, No. 51571101), the “Thirteenth Five-year Plan” Science & Technology Research Foundation of Education Bureau of Jilin Province, China (Grant No. 2015-479), NNSFC (No. 51501176) and the Project 985-High Properties Materials of Jilin University.

Author Contributions: Feng Qiu and Qi-Chuan Jiang conceived and designed the experiments; Feng Qiu, Xiang Gao, Jian Tang, Yu-Yang Gao and Qiang Li performed the experiments; Feng Qiu, Jian Tang, Shi-Li Shu, and Xue Han, analyzed the data; Feng Qiu wrote the paper.

Conflicts of Interest: The authors declare no conflict of interest.

References

1. Wang, L.; Qiu, F.; Ouyang, L.C.; Wang, H.Y.; Zha, M.; Shu, S.L.; Zhao, Q.L.; Jiang, Q.C. A novel approach of using ground CNTs as the carbon source to fabricate uniformly distributed nano-sized TiC_x/2009Al composites. *Materials* **2015**, *8*, 8839–8849. [[CrossRef](#)]
2. Zhao, Q.; Liang, Y.H.; Zhang, Z.H.; Li, X.J.; Ren, L.Q. Study on the impact resistance of bionic layered composite of TiC–TiB₂/Al from Al–Ti–B₄C System. *Materials* **2016**, *9*, 708. [[CrossRef](#)]
3. Shu, S.L.; Yang, H.Y.; Tong, C.C.; Qiu, F. Fabrication of TiC_x–TiB₂/Al composites for application as a Heat Sink. *Materials* **2016**, *9*, 642. [[CrossRef](#)]
4. Zhao, Q.; Liang, Y.H.; Zhang, Z.H.; Li, X.J.; Ren, L.Q. Microstructure and dry-sliding wear behavior of B₄C ceramic particulate reinforced Al 5083 matrix composite. *Metals* **2016**, *6*, 227. [[CrossRef](#)]
5. Sajjadi, S.A.; Ezatpoura, H.R.; Torabi Parizi, M. Comparison of microstructure and mechanical properties of A356 aluminum alloy/Al₂O₃ composites fabricated by stir and compo-casting processes. *Mater. Des.* **2012**, *34*, 106–111. [[CrossRef](#)]
6. Molina, J.M.; Prieto, R.; Narciso, J.; Louis, E. The effect of porosity on the thermal conductivity of Al–12 wt. % Si/SiC composites. *Scr. Mater.* **2009**, *60*, 582–585. [[CrossRef](#)]
7. Kerti, I.; Toptan, F. Microstructural variations in cast B₄C-reinforced aluminium matrix composites (AMCs). *Mater. Lett.* **2008**, *62*, 1215–1218. [[CrossRef](#)]

8. Du, X.F.; Gao, T.; Liu, G.L.; Liu, X.F. In situ synthesizing SiC particles and its strengthening effect on an Al-Si-Cu-Ni-Mg piston alloy. *J. Alloy. Compd.* **2017**, *695*, 1–8. [[CrossRef](#)]
9. Schöbel, M.; Altendorfer, W.; Degischer, H.P.; Vaucher, S.; Buslaps, T.; di Michiel, M.; Hofmann, M. Internal stresses and voids in SiC particle reinforced aluminum composites for heat sink applications. *Compos. Sci. Technol.* **2011**, *71*, 724–733. [[CrossRef](#)]
10. Xiong, B.; Xu, Z.; Yan, Q.; Cai, C.; Zheng, Y.; Lu, B. Fabrication of SiC nanoparticulates reinforced Al matrix composites by combining pressureless infiltration with ball-milling and cold-pressing technology. *J. Alloy. Compd.* **2010**, *497*, L1–L4. [[CrossRef](#)]
11. Kang, Y.C.; Chan, S.L.I. Tensile properties of nanometric Al₂O₃ particulate-reinforced aluminum matrix composites. *Mater. Chem. Phys.* **2004**, *85*, 438–443. [[CrossRef](#)]
12. Xiong, B.; Xu, Z.; Yan, Q.; Lu, B.; Cai, C. Effects of SiC volume fraction and aluminum particulate size on interfacial reactions in SiC nanoparticulate reinforced aluminum matrix composites. *J. Alloy. Compd.* **2011**, *509*, 1187–1191. [[CrossRef](#)]
13. Hsu, C.J.; Chang, C.Y.; Kao, P.W.; Ho, N.J.; Chang, C.P. Al–Al₃Ti nanocomposites produced in situ by friction stir processing. *Acta Mater.* **2006**, *54*, 5241–5249. [[CrossRef](#)]
14. Zhang, H.; Geng, L.; Guan, L.; Huang, L. Effects of SiC particle pretreatment and stirring parameters on the microstructure and mechanical properties of SiC_p/Al–6.8Mg composites fabricated by semi-solid stirring technique. *Mater. Sci. Eng. A* **2010**, *528*, 513–518. [[CrossRef](#)]
15. Mazahery, A.; Shabani, M.O. Characterization of cast A356 alloy reinforced with nano SiC composites. *Trans. Nonferr. Met. Soc. China* **2012**, *22*, 275–280. [[CrossRef](#)]
16. Dehghan Hamedan, A.; Shahmiri, M. Production of A356–1 wt % SiC nanocomposite by the modified stir casting method. *Mater. Sci. Eng. A* **2012**, *556*, 921–926. [[CrossRef](#)]
17. Nie, K.B.; Wang, X.J.; Wu, K.; Xu, L.; Zheng, M.Y.; Hu, X.S. Processing, microstructure and mechanical properties of magnesium matrix nanocomposites fabricated by semisolid stirring assisted ultrasonic vibration. *J. Alloy. Compd.* **2011**, *509*, 8664–8669. [[CrossRef](#)]
18. Mazahery, A.; Abdizadeh, H.; Baharvandi, H.R. Development of high-performance A356/nano-Al₂O₃ composites. *Mater. Sci. Eng. A* **2009**, *518*, 61–64. [[CrossRef](#)]
19. Tahamtan, S.; Halvae, A.; Emamy, M.; Zabihi, M.S. Fabrication of Al/A206–Al₂O₃ nano/micro composite by combining ball milling and stir casting technology. *Mater. Des.* **2013**, *49*, 347–359. [[CrossRef](#)]
20. Amirkhanlou, S.; Niroumand, B. Effects of reinforcement distribution on low and high temperature tensile properties of Al356/SiC_p cast composites produced by a novel reinforcement dispersion technique. *Mater. Sci. Eng. A* **2011**, *528*, 7186–7195. [[CrossRef](#)]
21. Yang, Y.; Lan, J.; Li, X. Study on bulk aluminum matrix nano-composite fabricated by ultrasonic dispersion of nano-sized SiC particles in molten aluminum alloy. *Mater. Sci. Eng. A* **2004**, *380*, 378–383. [[CrossRef](#)]
22. Zhao, H.L.; Yao, D.M.; Qiu, F.; Xia, Y.M.; Jiang, Q.C. High strength and good ductility of casting Al-Cu alloy modified by Pr_xO_y and La_xO_y. *J. Alloy. Compd.* **2011**, *509*, L43–L46. [[CrossRef](#)]
23. Xia, Y.M.; Bai, Z.H.; Qiu, F.; Jin, S.B.; Jiang, Q.C. Effects of multi-modification of rare earth oxides Pr_xO_y and La_xO_y on microstructure and tensile properties of casting Al-Cu alloy. *Mater. Sci. Eng. A* **2012**, *558*, 602–606. [[CrossRef](#)]
24. Kobashi, M.; Choh, T. Effects of alloying elements on SiC dispersion in liquid aluminum. *Mater. Trans.* **1990**, *12*, 1101–1107. [[CrossRef](#)]

